Journal of Physics:
Conference Series

PURPOSE-LED PUBLISHING™

PAPER • OPEN ACCESS

Simultaneous Modal Analysis and Fatigue Testing of Wind Turbine Rotor Blades

To cite this article: Kevin Gnebner *et al* 2026 *J. Phys.: Conf. Ser.* **3224** 062060

View the article online for updates and enhancements.

You may also like

- Research sized wind turbine blade modal tests: comparison of the impact excitation with shaker excitation
M. M. Luczak, B. Peeters, S. Manzato et al.
- Long-Term Tower Dynamic Tracking of 4.2MW Turbines from the WiValdi Research Wind Farm: First Results
Leon Liesecke, Clemens Jonscher, Tanja Grießmann et al.
- On the parameter sensitivity in structural parameter identification using Eigensystem Realization Algorithm for a MW-size wind turbine
Sho Oh and Takeshi Ishihara

Enabling Electrochemistry Inside and Outside the Lab

PalmSens

Discover our diverse range of Potentiostats engineered to support your research wherever it takes you

- Intuitive software for Windows and Android
- Proven in over 4000 scientific publications
- Single-channel and multi-channel
- Benchtop, portable and wearable

Discover More



This content was downloaded from IP address 129.247.247.240 on 05/11/2026 at 13:22

Simultaneous Modal Analysis and Fatigue Testing of Wind Turbine Rotor Blades

Kevin Gnebner[1], Giulia Jelicic[1], and Yves Govers[1]

[1]Institute of Aeroelasticity, German Aerospace Center (DLR), Göttingen, Germany

E-mail: kevin.gnebner@dlr.de

Abstract. This paper shows a structural health monitoring procedure for rotor blade fatigue testing without stopping the test for inspection. In detail it is demonstrated how modal analysis and fatigue testing of wind turbine rotor blades can be perfomed simultaneously. The proposed method was validated using a 12.6 m rotor blade equipped with 24 accelerometers. An imbalance fatigue exciter was positioned at $R = 7.8$ m to drive the blade at its first flapwise eigenfrequency of 1.83 Hz. This setup was supplemented by an additional electrodynamic shaker at $R = 3.5$ m to excite the rotor blade above the first flapwise eigenfrequency. The acceleration data of this combined excitation was then analyzed to determine the modal parameters (eigenfrequencies, damping ratios, and mode shapes). By comparing these results to a reference measurement (taken with the fatigue exciter switched off), it was found that system identification remains possible even despite the dominant sinusoidal excitation of the fatigue exciter. In total, 11 modes were compared in a frequency range of 3 to 50 Hz. The measured eigenfrequencies deviated by no more than 3.7% from the reference, though the damping values showed significantly higher scatter of up to 69%. A comparison of the mode shapes using the MAC matrix reveals a high correlation. Additionally, it was shown which aspects must be considered in such a test setup and which challenges may arise in the system identification. The main advantage of this procedure is that an already time-consuming fatigue test does not need to be interrupted for inspection purposes, and potential damage can be identified through changes in the modal parameters during the ongoing fatigue test.

1. Introduction

The global shift toward a more sustainable energy supply has established wind power as one of the most important pillars of renewable energy. As the rated power of modern wind turbines continues to increase, so do the dimensions of their rotor blades, which today can reach lengths of over 100 m. These rotor blades must withstand complex and multidirectional loads throughout their entire operational lifetime. Given the required service life of 20 to 25 years and the critical importance of the rotor blade for overall system reliability, a precise understanding and validation of its long-term behavior under fatigue loading is of crucial relevance. Fatigue testing of rotor blades is therefore an indispensable element of the development and certification process. It serves to ensure the structural integrity and reliability of the blade over its entire lifetime and to identify critical design weaknesses at an early stage. These tests are typically conducted as full-scale fatigue tests in which the blade is subjected to representative operational loads. In current standard fatigue tests, blades are tested consecutively in the flapwise and

Content from this work may be used under the terms of the Creative Commons Attribution 4.0 licence. Any further distribution of this work must maintain attribution to the author(s) and the title of the work, journal citation and DOI.
Published under licence by IOP Publishing Ltd

edgewise directions, with the test cycles typically set to 1 million for flapwise and 2 million for edgewise [1]. The overall duration of such full-scale fatigue tests is significantly influenced by a wide range of technical and organizational factors. A central aspect are the decreasing eigenfrequencies associated with increasing blade length, which lead to substantially longer testing times. In addition, extensive inspection and documentation phases – required to detect local damage, delamination, or material fatigue – further increase the total test duration. Logistical challenges, such as coordinating large test rigs, transporting exceptionally long blades also affect the schedule. Overall, this results in a demanding interplay of structural-dynamic, safety-related, and process-dependent factors that determine how long a fatigue test can realistically be carried out. According to Fraunhofer Institute for Wind Energy Systems (IWES) [2], the test duration for wind turbine rotor blades has increased significantly, rising from about one year for 90 m blades to roughly two years of testing for 115 m+ blades. In view of these time-consuming challenges, it becomes clear that traditional testing methods are reaching their limits and that new approaches are necessary to ensure the efficiency, reliability, and cost-effectiveness of these tests.

One of the most significant improvements in recent years in the field of fatigue testing of wind turbine rotor blades has been the development of multiaxial test rigs [3–7], which allow rotor blades to be tested simultaneously in both flapwise and edgewise directions. Since these tests are usually conducted separately, combining the two scenarios not only reduces testing time but also enables the introduction of more realistic loads. This increases the quality and validity of the experimental validation and reduces uncertainties in the design.

Another approach for significantly reducing testing time is the so-called segment blade test. Instead of testing the entire rotor blade as a whole, it is divided into several sections that are tested separately. Dividing the rotor blade into segments increases the eigenfrequencies of the test specimens, which in turn reduces the overall testing time. Numerical simulations presented in [8] showed that this segmented approach can reduce testing time by up to 43 and 52% for 60 and 90 m rotor blades. In addition, it is common practice to cut off the rotor blade tip to shorten the blade and thus to slightly increase the eigenfrequencies. IEC 61400-23 does not prohibit this procedure as long as it can be demonstrated that the fatigue life verification remains valid for all relevant sections of the blade.

In order to avoid time-consuming visual inspections before, during, and after fatigue tests, methods have been developed that enable early detection of potential damage and defects through measurement data. [9] presented how multiple artificial damages were monitored during a fatigue test using various sensing systems. Part of the instrumentation included classical accelerometers and an electrodynamic shaker to track the progress of damage based on changes in power spectral densities (PSDs) in a frequency range of 100 to 3,000 Hz. The key point here was that the shaker was only switched on for the estimation of the PSDs when the fatigue exciter was switched off. However, if it is possible to use the additional vibration shaker during the ongoing fatigue test to determine the modal parameters, the fatigue test could run without interruptions. That could save additional time, as such inspections can take several days.

Based on previously conducted research in modal testing — at both the component level for rotor blades [10, 11] and the global level for the entire wind turbine [12] — we aim to close this gap by presenting a new methodology that makes it possible to determine the modal parameters (and therefore potential changes in the structural integrity) of rotor blades using a vibration shaker and pre-installed accelerometers without stopping the ongoing fatigue test. We believe that by doing so, we can make a small contribution towards enabling faster execution of future fatigue tests for XXL rotor blades.

2. Test setup

The following sections outline the conditions under which the measurement campaign for validating the method was carried out. They describe the type of rotor blade used for the test, the sensor setup installed to measure the data, and the vibration exciters applied to generate the states required for the fatigue and modal test. The work and results presented here were conducted within the scope of HYBRID WIND project.



Figure 1. CAD overview of the test setup. The 12.6 m rotor blade is mounted on the test rig with the pressure side facing upwards. The yellow box represents the imbalance fatigue exciter, which is mounted at a radius of $R = 7.8$ m.

2.1. Rotor blade

For this test campaign, a 12.6 m glass fiber–reinforced polymer rotor blade was available, which originally came from the research project ReliaBlade [13]. The structural design includes a glass-fiber spar cap with a constant width of 0.3 m, as well as two shear webs bonded to the spar cap. The blade is intended as a replacement option for older 150 kW turbines, and one key design requirement is that it can operate both as a pitch-controlled and a stall-regulated blade. Consequently, its design does not reflect the state-of-the-art for modern pitch-regulated blades, but it will be unique due to the comprehensive availability of data and measured characteristics. Detailed information on the design and construction of the rotor blade can be found in [14, 15]. For the execution of the test, the rotor blade was mounted pressure side up on a test stand at Gdańsk University of Technology. The blade was mounted at a height of about 1.5 m above the ground, measured to the center of the root diameter. A schematic CAD overview of the test setup can be seen in Fig. 1.

2.2. Sensor setup

A various number of different sensor types were installed to determine the structural and vibrational responses of the rotor blade. Table 1 summarizes which types of sensors were used and how many of each type were installed on the rotor blade. We selected the accelerometers specifically to withstand the accelerations produced by the fatigue exciter and shaker, ensuring they could reliably capture data up to the ±10 g range. To mount the accelerometers, custom 3D-printed adapters were designed to match the rotor blade's surface, ensuring global alignment across all sensors. All sensors were installed on the pressure side with data acquisition handled via Simcenter Scadas and Testlab. The signals were sampled at a rate of 200 Hz.

2.3. Fatigue exciter

An imbalance fatigue exciter was used to carry out pure flapwise fatigue testing at the blade's first flapwise eigenfrequency of 1.83 Hz. The exciter consists of an adjustable mass mounted on an arm of variable length, allowing the mass to be positioned at different radii relative to the axis of rotation. This arm is attached to a bearing assembly integrated into a gearbox and

Table 1. Overview of sensor types and quantities.

Sensor type	Number
ICP accelerometer	24
3D MEMS accelerometer	1
Strain gauge	20
Load sensor	2
Force bridge sensor	2
Temperature sensor	3
Force transducer	1

driven by a 1500 W AC servo-synchronous motor. The entire system is installed on a support frame equipped with pads shaped to match the rotor blade. An integrated planetary gearbox with bearing assembly is used, rated for radial forces up to 4 kN. The control system consists of a dedicated motor controller connected to a PLC and a control panel. The exciter's rotational speed can be controlled with an accuracy better than 0.01 Hz, allowing precise tuning to the rotor blade's first flapwise eigenfrequency. The exciter is concentrated over a span between 7500 and 8000 mm and is capable of displacing the rotor blade at the tip by up to ± 0.5 m. The additional mass of the fatigue exciter (approximately 102 kg) leads to a reduction in the rotor blade eigenfrequencies and also affects the damping ratios of the different mode shapes. In Fig. 2, one can see how the fatigue exciter is mounted on the rotor blade.

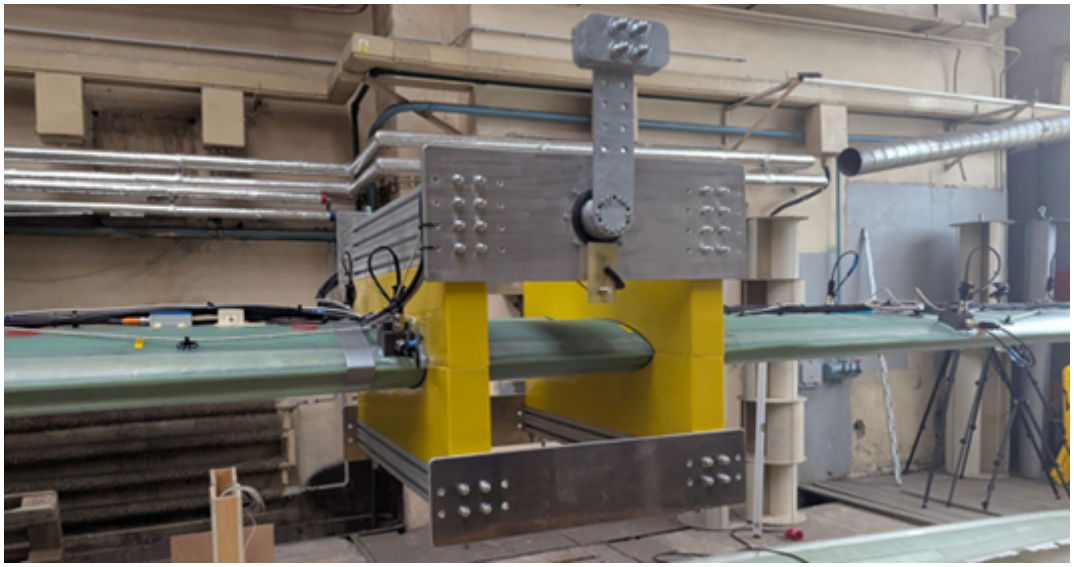


Figure 2. View of the imbalance fatigue exciter mounted on the rotor blade at radius $R = 7.8$ m.

2.4. Electrodynamic shaker

Since the fatigue exciter was intended to remain activated during this study, the blade's displacement had to be coordinated with the maximum stroke of the shaker. It was therefore necessary to ensure that the displacement at the position where the shaker would be mounted did not exceed the allowable stroke of the shaker. Consequently, this limited the possible installation position along the blade. To determine the optimal position, simulations based on the FE model were carried out to identify the maximum radial position at which the shaker could be installed

without causing the stroke to bottom out. In this case, an APS420 long stroke shaker with linear ball bearings from SPEKTRA was used, offering a stroke of 150 mm (peak-to-peak) and outputting up to 900 N between 0 and 200 Hz. The results showed that a radial position of $R = 3.5$ m was ideal for installing the shaker, taking into account an appropriate safety margin. The shaker was mounted at a 45° angle to the leading edge to excite modes in both flapwise and edgewise directions. A picture of the shaker installed on the rotor blade is shown in Fig. 3.



Figure 3. Picture of the APS420 long stroke shaker from SPEKTRA, installed on the rotor blade at $R = 3.5$ m.

2.5. Excitation signals

A key consideration was that the additional excitation signal had to be superimposed on the dominant harmonic excitation of the fatigue exciter. This established the requirement that the additional excitation signal had to introduce sufficient energy into the structure to excite all other vibration modes, besides the 1st flapwise mode. Therefore, a total of three different excitation signals were generated and tested to determine which one would perform best for this purpose:

- Random signal,
- crest-optimized random signal, and
- swept-sine signal.

All three signals had a frequency content between 2.5 and 80 Hz. When selecting the frequency content of the individual signals, particular care was taken to ensure that the lower bound of the frequency content lies above the first flapwise eigenfrequency of 1.83 Hz. The additional excitation is intended solely to excite mode shapes above the first flapwise mode. For each of the two random excitations, a 10-minute signal was generated. A crest factor of CF = 1.6 was chosen for the crest-optimized random signal. The duration of the swept-sine signal was

determined by the frequency content and sweep rate of 0.5 oct/min. Figure 4 shows the signals of the force transducer for the different excitations.

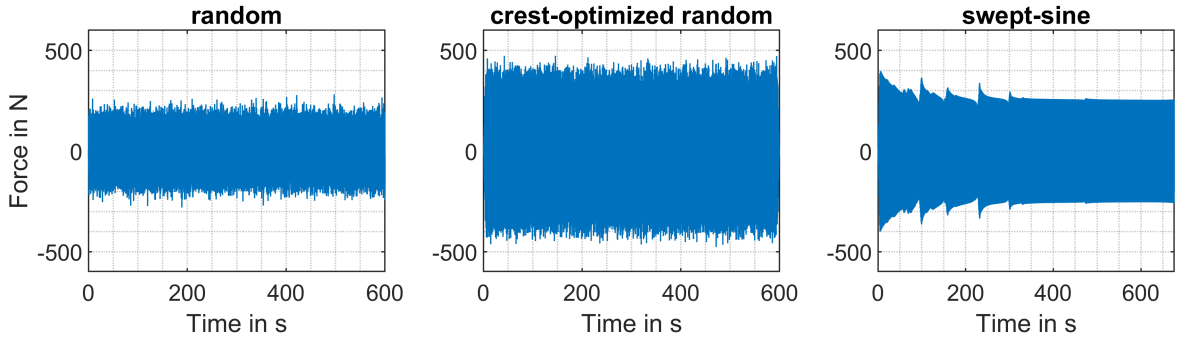


Figure 4. Three measured force signals (from left to right): random, crest-optimized random, and swept sine.

3. Modal analysis

3.1. Finite element analysis

To determine optimal positions of the accelerometers for modal analysis, a finite element analysis (FEA) was conducted in MSC Nastran (SOL 103 – dynamic response). A total of 20 mode shapes were calculated in a frequency range of 2 to 100 Hz. These results were post-processed in MATLAB®. Due to the level of detail and the size of the FE model (approx. $2.4 \cdot 10^6$ degrees of freedom), a model reduction to about 200 degrees of freedom was performed. These results formed the basis for the subsequent distribution of the accelerometers on the actual rotor blade. The goal in selecting the sensor positions was to determine locations that would allow all subsequent mode shapes in the real test to be sufficiently well identifiable. The so-called MAC (Modal Assurance Criterion) matrix was calculated to quantify this approach. After several iterations, a measurement setup comprising 24 accelerometers was established, distributed across a total of eight cross-sections. At each cross-section, three sensors were placed: two sensors at the leading edge (edge X, flap Y) and one sensor at the trailing edge (flap Y), see Fig. 5. Installing two sensors in Y-direction per cross-section enables the identification of torsional modes. It should be noted that the additional mass of the fatigue exciter was not taken into account in the simulations, which is why the eigenfrequencies deviate slightly from the actual ones.

3.2. Reference data

For the modal test, the measurement data from the 24 accelerometers were used. As a first step, a reference dataset of the rotor blade including the additional mass of the fatigue exciter was recorded with the fatigue exciter switched off. The results of the modal identification served as the basis for comparison with the results obtained using the methodology presented in this study. The rotor blade was excited by a crest-optimized random signal. For modal identification, the well-known frequency-domain method LSCF [16] was used. The results of the reference measurement are shown in Tab. 2. In a frequency range of 1.8 to 50 Hz, a total of 12 mode shapes were identified.

3.3. Validation of methodology

Based on the preparations and the reference dataset, the fatigue exciter was then switched on. Therefore, the rotor blade was excited by a combination of the mono-frequency excitation

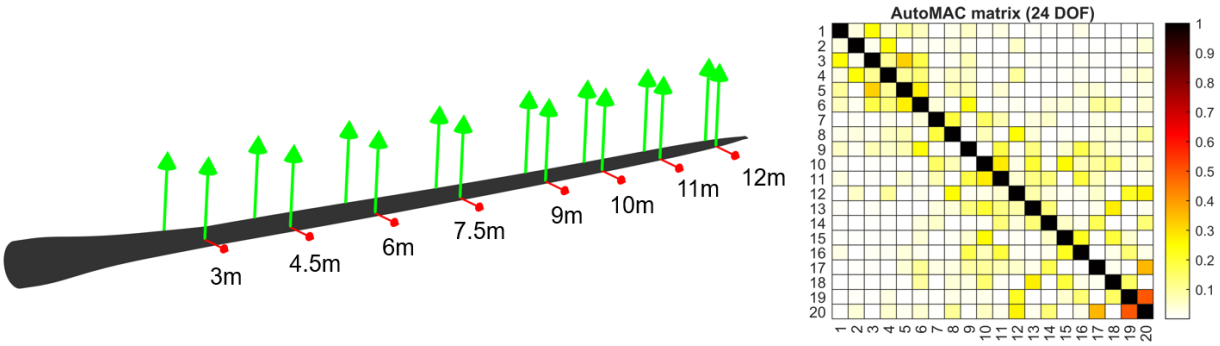


Figure 5. Sensor setup of the 24 accelerometers based on a finite element analysis (FEA), distributed across eight cross-sections with three sensors each. The corresponding AutoMAC matrix with the selected 24 degrees of freedom (DOF) shows that the first 20 mode shapes can be clearly distinguished from each other.

from the fatigue exciter and an excitation signal from the vibration shaker. For reasons of clarity and conciseness, a detailed treatment of the results obtained with the different excitation signals is not provided here, as a crest-optimized random signal was found to yield the most reliable results. Figure 6 shows the recorded time data of this combined excitation. It can be seen clearly that the mono-frequency signal is superimposed with random. These 10-minute recordings were then used to identify the modal parameters of the rotor blade. When applying

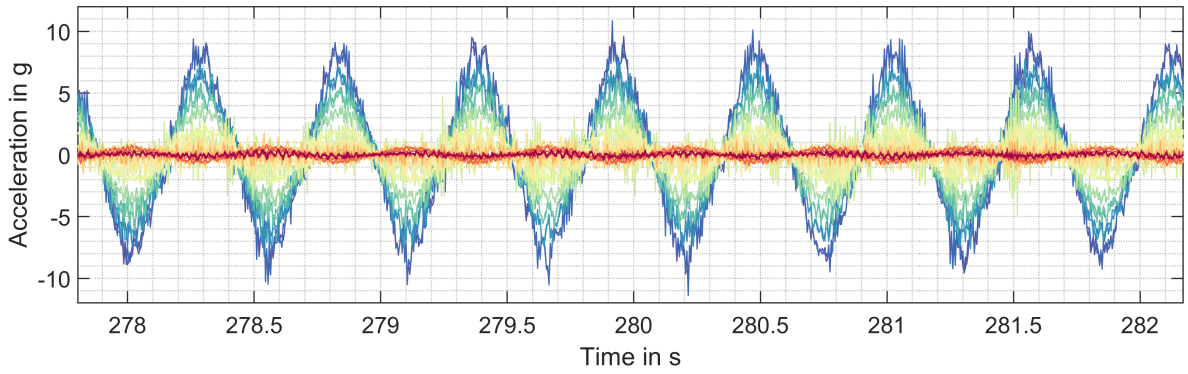


Figure 6. Time data window of the 24 accelerometers during fatigue and shaker excitation.

system identification methods, it is common to use frequency bands around resonance peaks. In this case, it is particularly important that no frequency band is set around the resonance of the first flapwise mode, which is excited by the fatigue exciter. This resonance peak must be ignored during the analysis, otherwise, the system identification is not successful. For the present application, the first frequency band was selected starting at 2.5 Hz. The results of the identification are also listed in Tab. 2. Taking a look at the eigenfrequencies one sees that both scenarios yield very similar results. Even with the large blade displacements and the combined excitation, we were able to reproduce the eigenfrequencies with high precision — with a maximum deviation of 3.7%. In all cases, the eigenfrequencies are slightly lower when the fatigue exciter is active. However, a comparison of the damping values shows a different result. The damping values deviate significantly from the reference measurement results which can be explained by two main factors: first, aerodynamic effects (and therefore aerodynamic

Table 2. Comparison of modal results under crest-optimized random excitation (fatigue exciter off/on).

No	Mode	Fatigue exciter off		Fatigue exciter on		Deviation	
		f in Hz	ζ in %	f in Hz	ζ in %	f in %	ζ in %
1	1st flap	1.833	0.300	–	–	–	–
2	1st edge	3.116	0.387	3.108	0.442	−0.235	12.462
3	2nd flap	5.420	0.250	5.417	0.799	−0.058	68.735
4	2nd edge	11.754	0.538	11.581	0.612	−1.492	12.150
5	1st torsion	12.409	0.592	12.407	1.130	−0.012	47.586
6	3rd flap	14.649	0.509	14.620	1.145	−0.200	55.513
7	4th flap	21.744	0.761	21.737	1.015	−0.032	24.989
8	3rd edge	29.772	1.517	29.572	1.723	−0.676	11.935
9	5th flap	33.617	1.201	33.104	2.034	−1.550	40.942
10	6th flap	41.267	1.670	39.786	2.356	−3.721	29.106
11	4th edge	44.653	1.941	43.152	2.177	−3.478	10.826
12	7th flap	47.011	1.596	46.860	2.100	−0.321	23.975

damping) caused by the large deflections of the rotor blade play a non-negligible role; second, the operation of the fatigue exciter itself introduces additional damping to the system. In all cases, the damping values are significantly higher when the fatigue exciter is active. The MAC matrix shown in Fig. 7 gives additional information about the deviation of modal parameters in terms of mode shapes between fatigue exciter off and on data. It can be seen that the mode shapes are highly correlated between the two test scenarios.

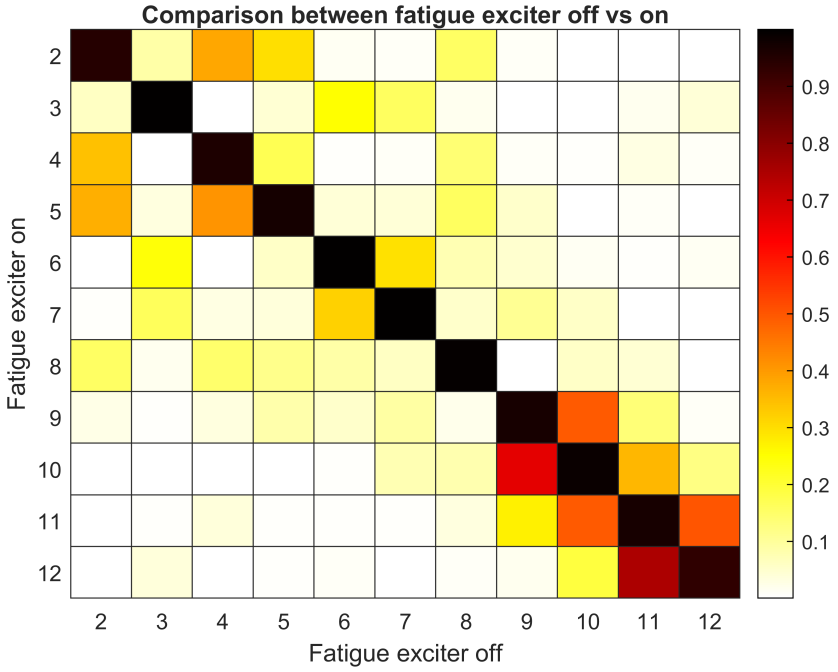


Figure 7. MAC matrix between fatigue exciter off and on.

3.4. From lab-scale to full-scale testing

In this test campaign, the scaled 12.6 m rotor blade was positioned 1.5 m above the ground. This allowed the vibration exciter to be placed directly on the floor and adjusted via the shaker frame's feet, making the attachment to the blade straightforward. In full-scale tests, however, this approach is not feasible, as the center of the blade root is typically mounted on a test rig at a height of 5–10 m above ground level. One possible solution is to position the shaker on a tower-like support structure in order to bridge the vertical distance between the ground and the rotor blade. We (DLR) have already implemented such a configuration during a modal test of a 56 m rotor blade on a test rig, see Fig. 8 (left). If no tower structures are available, or if the

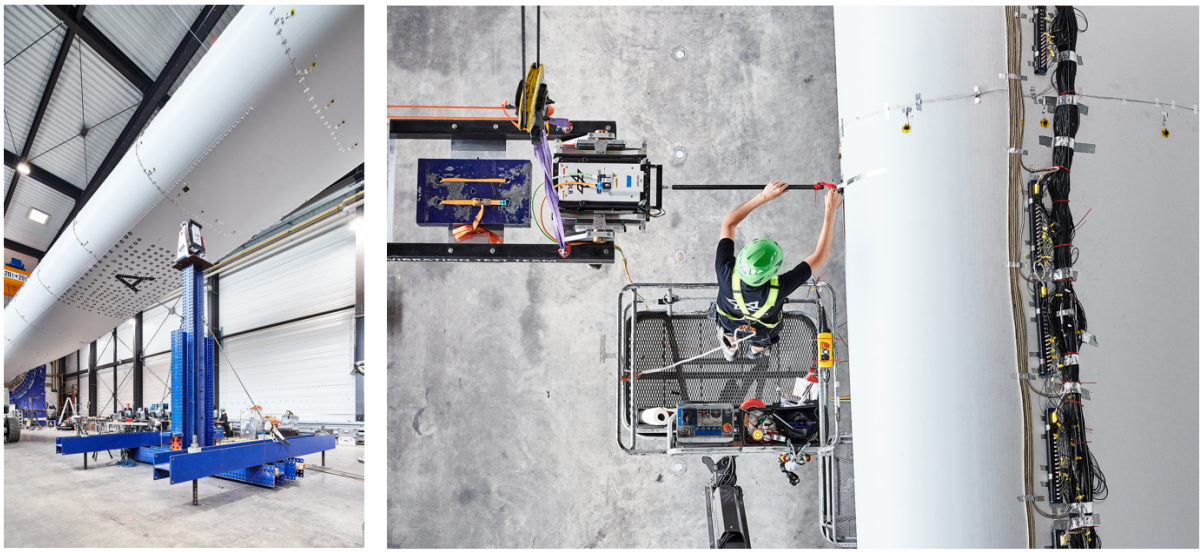


Figure 8. Positioning of shakers for a modal test of a 56 m rotor blade on a test rig. Left: The shaker was mounted on a tower-like structure to bridge the distance between the rotor blade and the hall floor. Right: The vibration exciter, including its frame and additional masses, was attached to the existing overhead crane in order to bring the shaker into position. The tests were carried out in the test hall of Fraunhofer IWES in Bremerhaven in 2022.

vertical distance between the ground and the rotor blade cannot be bridged using such towers, a second approach is to suspend the vibration exciter from an overhead crane in order to position the shaker at the required location. This configuration was also implemented during the same modal test, see Fig. 8 (right). In both cases, the excitation force was introduced to the rotor blade via a long stinger. In future tests, the shaker's position and stroke must also be matched to the expected displacement of the rotor blade.

Theoretically, a second shaker is not strictly necessary, provided that the fatigue exciter or the hydraulic actuators can also be used to excite the rotor blade in the higher frequency range. This would allow for the application of a superimposed signal consisting of a sinusoidal and random component (Sine-On-Random). By integrating the modal excitation into the existing fatigue test setup, both loading conditions could be induced through a single actuation system, thereby eliminating the need for an additional shaker.

4. Conclusions and outlook

By selecting an appropriate shaker, it is possible to excite the rotor blade in the higher frequency range during an ongoing fatigue test, even despite the large deflections. The shaker's stroke

capacity needs to be coordinated with the blade's displacement to ensure it does not reach its mechanical limits. Furthermore, the choice of excitation signal is crucial: it must provide enough energy to the structure to overcome the dominant influence of the fatigue exciter at the first flapwise frequency. The results of this campaign demonstrate that system identification remains reliable. The eigenfrequencies were reproduced with high precision compared to the reference measurement. The damping values, however, deviate significantly due to aerodynamic effects and the operation of the fatigue exciter itself. In principle, these high deviations are negligible if the objective is simply to monitor for damage via modal parameter shifts. The damping values identified here represent a combination of structural and aerodynamic damping. Nevertheless, any change in damping caused by damage remains detectable with this method. Only a reference measurement of the healthy rotor blade is needed for comparison. Consequently, this method enables the detection of structural changes through changes in modal parameters during an ongoing fatigue test, eliminating the need for time-consuming interruptions.

The next phase of the project involves the construction of a new 12.6 m rotor blade based on the same design, but with intentional artificial damages embedded during the manufacturing process. This blade will then undergo a full fatigue test in a climate chamber at −20 °C to specifically investigate the influence of low temperatures on damage progression. As part of this measurement campaign, the method presented here will be applied, utilizing an additional shaker to detect real structural changes through changes in modal parameters during the ongoing fatigue test. Therefore, an online monitoring procedure will be set up to track the modes during fatigue test fully autonomously. Any changes in the structural dynamics behavior indicating damage can then be identified without stopping the fatigue test.

Acknowledgements

This research was funded by CETPartnership, the Clean Energy Transition Partnership under the 2022 joint call for research proposals, co-funded by the European Commission (GA N°101069750) and with the funding organizations detailed on https://cetpartnership.eu/funding-agencies-and-call-modules. This research was also funded by the German Federal Ministry for Economic Affairs and Energy (FKZ 03EE3102A). The authors would like to thank all participants of this measurement campaign for their contributions. This publication would not have been possible without their untiring support.



References

[1] Yoon S H, Kim J, Kim K D, Park J and Moon J B 2023 Fatigue evaluation test method using the inertia generator for the ultra-large offshore wind turbine blade *Ocean Engineering* **280** 114802

[2] de Vries E 2023 Exclusive: Fraunhofer iwes unveils 115-metre-plus blade test rig for large wind turbine rotor blades URL `https://www.windpowermonthly.com/article/1828752/exclusive-fraunhofer-iwes-unveils-115-metre-plus-blade-test-rig-large-wind-turbine-rotor-blades`

[3] Snowberg D, Dana S, Hughes S and Berling P 2014 Implementation of a biaxial resonant fatigue test method on a large wind turbine blade Tech. rep. National Renewable Energy Lab.(NREL), Golden, CO (United States)

[4] Post N and Bürkner F 2016 *Fatigue test design: Scenarios for biaxial fatigue testing of a 60-meter wind turbine blade* (National Renewable Energy Laboratory)

[5] Bürkner F 2020 *Biaxial dynamic fatigue tests of wind turbine blades* Ph.D. thesis , Leibniz University Hannover, Hannover, Germany

[6] Melcher D, Bätge M and Neßlinger S 2020 A novel rotor blade fatigue test setup with elliptical biaxial resonant excitation *Wind Energy Science* **5** 675–684

[7] Castro O, Belloni F, Stolpe M, Yeniceli S C, Berring P and Branner K 2021 Optimized method for multi-axial fatigue testing of wind turbine blades *Composite Structures* **257** 113358

[8] Ha K, Bätge M, Melcher D and Czichon S 2020 Development and feasibility study of segment blade test methodology *Wind Energy Science* **5** 591–599

[9] Fremmelev M A, Ladpli P, Orlowitz E, Bernhammer L O, McGugan M and Branner K 2022 Structural health monitoring of 52-meter wind turbine blade: Detection of damage propagation during fatigue testing *Data-Centric Engineering* **3** e22

[10] Gundlach J and Govers Y 2019 Experimental modal analysis of aeroelastic tailored rotor blades in different boundary conditions *Journal of Physics: Conference Series* vol 1356 (IOP Publishing) p 012023

[11] Govers Y, Gnebner K, Kober P and Jelicic G 2025 Reliable damping ratio estimates from a 50m+ wind turbine rotor blade as a guide for prototype testing in the low frequency regime *11th International Operational Modal Analysis Conference*

[12] Gnebner K and Govers Y 2024 Operational modal analysis of the idling cart3 research wind turbine using bladevision data *International Operational Modal Analysis Conference* (Springer) pp 638–648

[13] Sayer F, Antoniou A, Goutianos S, Gebauer I, Branner K and Balzani C 2020 Reliablade project: A material's perspective towards the digitalization of wind turbine rotor blades *IOP Conference Series: Materials Science and Engineering* vol 942 (IOP Publishing) p 012006

[14] Haselbach P U, Zahle F, Berring P, Semenov S, Voltá L, Roqueta I and Verelst D R 2020 Blade research and demonstration platform *Journal of Physics: Conference Series* vol 1618 (IOP Publishing) p 052073

[15] Haselbach P U, Semenov S and Berring P 2020 Dtu's blade research and demonstration platform *IOP Conference Series: Materials Science and Engineering* vol 942 (IOP Publishing) p 012043

[16] Schoukens J, Rolain Y, Gustafsson F and Pintelon R 1998 Fast calculation of least-squares estimates for system identification *Proceedings of the 37th IEEE Conference on Decision and Control (Cat. No. 98CH36171)* vol 3 (IEEE) pp 3408–3410